Available online at www.sciencedirect.com
SCIENCE DIRECT®
International Journal of Heat and Mass Transfer 47 (2004) 459–476
International Journal of HEAT and MASS TRANSFER
www.elsevier.com/locate/ijhmt

Heat transfer flow in a parallel-plate channel by inserting in parallel impermeable sheets for multi-pass coolers or heaters

Chii-Dong Ho *, Yu-Chuan Tsai, Jr-Wei Tu

Department of Chemical Engineering, Tamkang University, Tamsui, 251 Taipei, Taiwan, ROC

Received 23 March 2003; received in revised form 25 July 2003

Abstract

The influences of recycle at the ends on multi-pass coolers or heaters through a parallel-plate channel with constant wall temperature are studied and an exact solution of this problem is presented using an orthogonal expansion technique. Analytical results show that the external refluxes can enhance the heat transfer efficiency due to the desirable convective effect having more influence than the undesirable preheating effect for all Graetz numbers, leading to considerably improved device performance in heat transfer. The results are represented graphically and compared with the heat transfer efficiency by the adjustment of channel thickness ratio in a single-pass operation (without inserting impermeable sheets). The suitable selections of the design and operating parameters on considering of both the heat transfer improvement and power consumption increment are also discussed.

1. Introduction

The problems of concerning steadily laminar forced convection heat or mass transfer in a bounded conduit with ignoring axial conduction or diffusion are the well-known Graetz problems [1,2]. Some researchers had further extended the classic Graetz problem to a variety of boundary conditions (with taking into account [3] or ignoring [4,5] axial conduction) and to multi-phase or multi-stream systems [6–12], as referred to conjugated Graetz problems, in an effort to simulate physical situations more directly. Beyond the initial concern for the single-stream problem, developments in the theoretical formulation of multi-stream systems have yielded analytical descriptions of multi-pass operations which couple through mutual conditions at the boundaries [13–16].

Internal or external reflux always plays a significant role on heat transfer and has received a great deal of attention in the literature. It is natural to speculate on the applicability of these effects to absorption, fermentation and polymerization, which are used extensively in loop reactors [17,18], air-lift reactors [19,20] and draft-tube bubble columns [21,22].

In the present paper, the problem of heat transfer in coolers or heaters, for fully developed laminar flow in a parallel plate divided into a multi-stream operation by inserting the parallel impermeable sheets with external refluxes, has been worked out exactly, including the effects of recycle ratio and impermeable-sheet position. The walls of the parallel plate are kept at a constant temperature and the fluid enters the parallel plate at different temperatures. The simultaneous differential equations governing the problem are then treated using an orthogonal expansion technique. This technique was employed successfully in solving conjugated Graetz problems by many investigators [23–27]. Without loss of generality, eigenfunctions are expressed to be polynomials with expansion coefficients containing the characteristic parameter, which is solved by the orthogonality conditions. An exact solution of the problem on heat transfer of multi-pass flow in a parallel-plate device with external refluxes is given in Section 2. Due to the rapid convergence of the infinite series, the method of eigenfunction expansion technique with eigenfunction expanding in terms of an extended power series is

* Corresponding author. Tel.: +886-2621-5656; fax: +886-2620-9887.
E-mail address: cdho@mail.tku.edu.tw (C.-D. Ho).

0017-9310/$ - see front matter © 2003 Elsevier Ltd. All rights reserved.
doi:10.1016/j.ijheatmasstransfer.2003.07.009

Nomenclature

B	conduit width, m
D_h	hydraulic diameter, m
F_m	eigenfunction associated with eigenvalue λ_m
Gz	Graetz number, $2VW/\alpha BL$
G_m	function defined during the use of orthogonal expansion method
$\overline{h}$	average heat transfer coefficient, kW/m^2 K
I_h	improvement of heat transfer, defined by Eq. (37)
I_p	increment of power consumption, defined by Eq. (38)
k	thermal conductivity of the fluid, kW/m K
L	conduit length, m
ℓw_f	friction loss in conduit, m^2/s^2
P	hydraulic dissipated energy
$\overline{Nu}$	Nusselt number
R	reflux ratio
S_m	expansion coefficient associated with eigenvalue λ_m
T	temperature of fluid, K
V	input volume flow rate of conduit, m^3/s
v	velocity distribution of fluid, m/s
$\overline{v}$	average velocity of fluid, m/s
W	distance between two parallel plates, m
x	transversal coordinate, m
z	longitudinal coordinate, m

Greek symbols

α	thermal diffusivity of fluid, m^2/s
β	ratio of channel thickness, $W_a/W_b = W_d/W_c$
η	transversal coordinate, x/W
θ	dimensionless temperature, $(T - T_I)/(T_s - T_I)$
λ_m	eigenvalue
μ	fluid viscosity, kg/m s
ξ	longitudinal coordinate, z/L
ρ	density of the fluid, kg/m^3
ψ	dimensionless temperature, $(T - T_s)/(T_I - T_s)$

Subscripts

a	in the channel a
b	in the channel b
c	in the channel c
d	in the channel d
F	at the outlet, $\xi = 0$
I	at the inlet
0	in a single-pass device without recycle
s	at the wall surface

employed to solve the multi-pass device in a more straightforward manner. The influences of sheet position and recycle ratio on the heat-transfer efficiency and power consumption increment for multi-pass operations are also determined to allow the specification set by designer. One may follow the analytic procedure performed in the present paper and develop a model for other conjugated Graetz problems in heat- and mass-transfer devices with many further possible boundary conditions in two or more contiguous streams and phases of multi-stream or multi-phase problems.

There are two purposes in the present study: first, to develop the theoretical formulation for multi-pass coolers or heaters by using the eigenfunction expansion technique; second, to investigate the heat-transfer efficiency improvement of such multi-pass coolers or heaters and to discuss the influence of the sheet position and recycle ratio on the device performance.

2. Mathematical formulations

2.1. Temperature distributions in multi-pass devices

An alternative design for increasing the heat transfer rate with the inlet fluid flow rate specified and kept unchanged. Three parallel impermeable sheets with negligible thickness and negligible thermal resistance are used in a parallel conduit of thickness W, length L, and width B ($>>W$) to divide it into four subchannels, subchannel a, b, c and d, with channel thickness W_a, W_b, W_c and W_d, respectively. The channel thickness ratio is defined as $\beta_{ab} = W_a/W_b$ and $\beta_{cd} = W_d/W_c$. Before entering each of two outer channels for a four-pass operation as shown in Fig. 1(a), the fluid with volumetric flow rate V and the inlet temperature T_I will mix with the fluid exiting from the inner channel with the volumetric flow rate RV and the outlet temperature $T_F = (T_{F,ab} + T_{F,cd})/2$, which is regulated using a conventional pump. The fluid is mixed completely at the inlet and outlet of each subchannel.

The theoretical analysis is developed through following assumptions: constant physical properties and wall temperature; purely fully developed laminar flow in each subchannel; negligible axial conduction as well as entrance length and end effects. After the following dimensionless variables are introduced:

$$\eta_i = \frac{x_i}{w_i}, \quad \xi = \frac{z}{L}, \quad \psi_i = \frac{T_i - T_s}{T_I - T_s}, \quad \theta_i = 1 - \psi_i = \frac{T_i - T_I}{T_s - T_I},$$
$$Gz = \frac{2V(W_a + W_b + W_c + W_d)}{\alpha BL} = \frac{2VW}{\alpha BL}, \qquad i = a, b, c, d \tag{1}$$

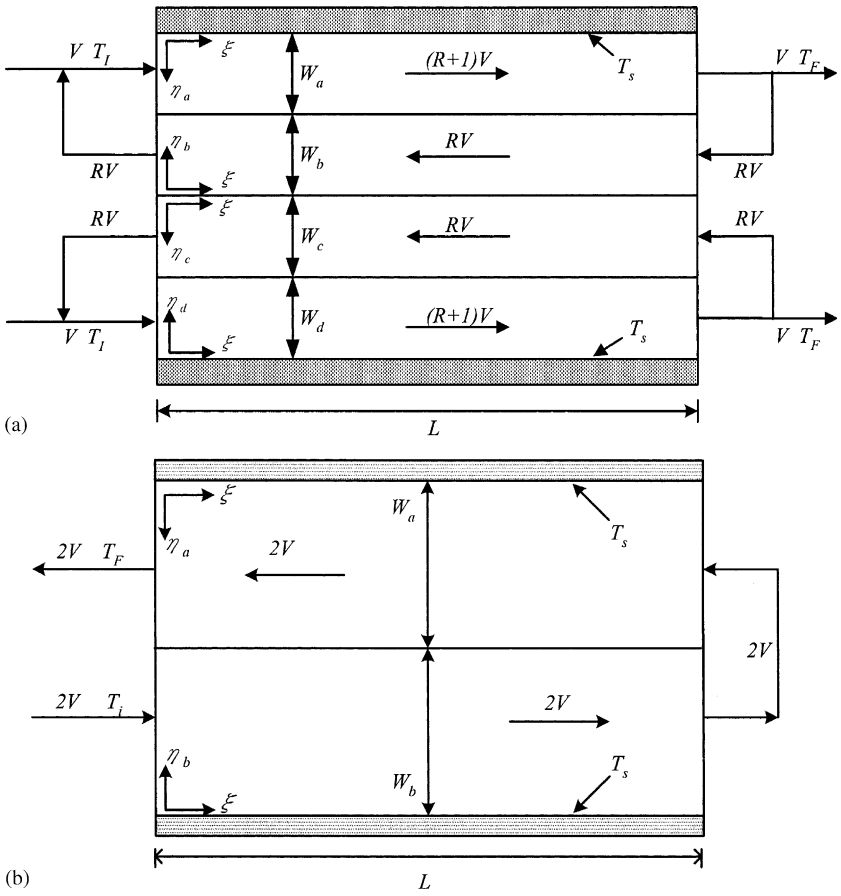

Fig. 1. (a) Multi-pass parallel-plate coolers or heaters with external refluxes at both ends. (b) Double-pass coolers or heaters.

The velocity distributions and equations of energy in dimensionless form may be obtained as

$$\frac{\partial^2\psi_i(\eta_i,\xi)}{\partial\eta_i^2}=\left[\frac{W_i^2 v(\eta_i)}{L\alpha}\right]\frac{\partial\psi_i(\eta_i,\xi)}{\partial\xi},\quad i=a,b,c,d \tag{2}$$

$$v_i(\eta_i)=\overline{v_i}(6\eta_i-6\eta_i^2),\quad 0\leqslant\eta_i\leqslant 1,\ \ i=a,b,c,d \tag{3}$$

in which $\overline{v_a}=[(R+1)V/W_aB]$, $\overline{v_b}=-[RV/W_bB]$, $\overline{v_c}=-[RV/W_cB]$, $\overline{v_d}=[(R+1)V/W_dB]$.

The boundary conditions used for solving Eqs. (2) and (3) are

$$\psi_a(0,\xi)=0 \tag{4}$$

$$\psi_a(1,\xi)=\psi_b(1,\xi) \tag{5}$$

$$-\frac{\partial\psi_a(1,\xi)}{\partial\eta_a}=\frac{W_a}{W_b}\frac{\partial\psi_b(1,\xi)}{\partial\eta_b} \tag{6}$$

$$\psi_b(0,\xi)=\psi_c(0,\xi) \tag{7}$$

$$-\frac{\partial\psi_b(0,\xi)}{\partial\eta_b}=\frac{W_b}{W_c}\frac{\partial\psi_c(0,\xi)}{\partial\eta_c} \tag{8}$$

$$\psi_c(1,\xi)=\psi_d(1,\xi) \tag{9}$$

$$-\frac{\partial\psi_c(1,\xi)}{\partial\eta_c}=\frac{W_c}{W_d}\frac{\partial\psi_d(1,\xi)}{\partial\eta_d} \tag{10}$$

$$\psi_d(0,\xi)=0 \tag{11}$$

and the dimensionless outlet temperature is

$$\theta_F=(\theta_{F,ab}+\theta_{F,cd})/2=1-(\psi_{F,ab}+\psi_{F,cd})/2=\frac{(T_{F,ab}+T_{F,cd})/2-T_I}{T_s-T_I} \tag{12}$$

By following the similar procedure performed in our previous work [15], the analytical solution to this problem will be obtained with the eigenfunctions expanding in terms of an extended power series. The dimensionless outlet temperature, referred to the bulk temperature, is obtained by making the overall energy balances on both outer subchannels. It was in terms of the Graetz number (Gz), eigenvalues (λ_m), expansion coefficients ($S_{a,m}$, $S_{b,m}$, $S_{c,m}$ and $S_{d,m}$), location of impermeable sheet (β_{ab} and β_{cd}) and eigenfunctions ($F_{a,m}$, $F_{b,m}$,

$F_{c,m}$ and $F_{d,m}$). The procedures for evaluating the eigenvalues and expansion coefficients are shown in Appendix A and the result is as follows:

$$\begin{aligned}\psi_{F,ab} &= \frac{-\int_0^1 v_b W_b B\psi_b(\eta_b,1)\,\mathrm{d}\eta_b}{VR}\\ &= \frac{-W}{W_b RGz}\sum_{m=0}^{\infty}\frac{S_{b,m}}{\lambda_m}\{F'_{b,m}(1)-F'_{b,m}(0)\}\\ &= \frac{\int_0^1 v_a W_a B\psi_a(\eta_a,1)\,\mathrm{d}\eta_a}{V(R+1)}\\ &= \frac{W}{W_a(R+1)Gz}\sum_{m=0}^{\infty}\frac{S_{a,m}}{\lambda_m}\{F'_{a,m}(1)-F'_{a,m}(0)\}\end{aligned}\tag{13}$$

or

$$\begin{aligned}\psi_{F,cd} &= \frac{-\int_0^1 v_c W_c B\psi_c(\eta_c,1)\,\mathrm{d}\eta_c}{VR}\\ &= \frac{-W}{W_c RGz}\sum_{m=0}^{\infty}\frac{S_{c,m}}{\lambda_m}\{F'_{c,m}(1)-F'_{c,m}(0)\}\\ &= \frac{\int_0^1 v_d W_d B\psi_d(\eta_d,1)\,\mathrm{d}\eta_d}{V(R+1)}\\ &= \frac{W}{W_d(R+1)Gz}\sum_{m=0}^{\infty}\frac{S_{d,m}}{\lambda_m}\{F'_{d,m}(1)-F'_{d,m}(0)\}\end{aligned}\tag{14}$$

or may be examined using Eq. (17), readily obtained from the following overall energy balance on the outer walls

$$\begin{aligned}&V(1-\psi_{F,ab})+V(1-\psi_{F,cd})\\ &\quad=\int_0^1\frac{\alpha BL}{W_a}\frac{\partial\psi_a(0,\xi)}{\partial\eta_a}\,\mathrm{d}\xi+\int_0^1\frac{\alpha BL}{W_d}\frac{\partial\psi_d(0,\xi)}{\partial\eta_d}\,\mathrm{d}\xi\end{aligned}\tag{15}$$

thus,

$$\begin{aligned}&(1-\psi_{F,ab})+(1-\psi_{F,cd})\\ &\quad=\frac{2}{Gz}\left[\sum_{m=0}^{\infty}S_{a,m}F'_{a,m}(0)\frac{(1-\mathrm{e}^{-\lambda_m})W}{\lambda_m W_a}\right.\\ &\qquad\left.+\sum_{m=0}^{\infty}S_{d,m}F'_{d,m}(0)\frac{(1-\mathrm{e}^{-\lambda_m})W}{\lambda_m W_d}\right]\end{aligned}\tag{16}$$

or

$$\begin{aligned}\psi_{F,ab}+\psi_{F,cd} = 2-\frac{2}{Gz}&\left[\sum_{m=0}^{\infty}S_{a,m}F'_{a,m}(0)\frac{(1-\mathrm{e}^{-\lambda_m})W}{\lambda_m W_a}\right.\\ &\left.+\sum_{m=0}^{\infty}S_{d,m}F'_{d,m}(0)\frac{(1-\mathrm{e}^{-\lambda_m})W}{\lambda_m W_d}\right]\end{aligned}\tag{17}$$

Once the eigenvalues and associated expansion coefficients are obtained, the dimensionless outlet temperature is readily calculated by Eq. (17). Also, the mixed inlet temperatures of both outer subchannels are calculated by

$$\begin{aligned}\psi_a(\eta_a,0) &= \frac{-\int_0^1 v_b W_b B\psi_b(\eta_b,0)\,\mathrm{d}\eta_b+V}{V(R+1)}\\ &= \frac{1}{R+1}\left[1-\frac{W}{W_b Gz}\sum_{m=0}^{\infty}\frac{S_{b,m}\mathrm{e}^{-\lambda_m}}{\lambda_m}\{F'_{b,m}(1)\right.\\ &\qquad\left.-F'_{b,m}(0)\}\right]\end{aligned}\tag{18}$$

and

$$\begin{aligned}\psi_d(\eta_d,0) &= \frac{-\int_0^1 v_c W_c B\psi_c(\eta_c,0)\,\mathrm{d}\eta_c+V}{V(R+1)}\\ &= \frac{1}{R+1}\left[1-\frac{W}{W_c Gz}\sum_{m=0}^{\infty}\frac{S_{c,m}\mathrm{e}^{-\lambda_m}}{\lambda_m}\{F'_{c,m}(1)\right.\\ &\qquad\left.-F'_{c,m}(0)\}\right]\end{aligned}\tag{19}$$

2.2. Temperature distributions in double-pass devices

Similarly, for the double-pass device as shown in Fig. 1(b), only an impermeable sheet is inserted to divide a parallel conduit into two subchannels, subchannel a and b. The equations of heat transfer in dimensionless form may be also obtained as

$$\frac{\partial^2\psi_a(\eta_a,\xi)}{\partial\eta_a^2}=\left[\frac{W_a^2 v_a(\eta_a)}{L\alpha}\right]\frac{\partial\psi_a(\eta_a,\xi)}{\partial\xi}\tag{20}$$

$$\frac{\partial^2\psi_b(\eta_b,\xi)}{\partial\eta_b^2}=\left[\frac{W_b^2 v_b(\eta_b)}{L\alpha}\right]\frac{\partial\psi_b(\eta_b,\xi)}{\partial\xi}\tag{21}$$

in which

$$\begin{aligned}&v_a(\eta_a)=\frac{V}{W_a B}(6\eta_a-6\eta_a^2),\quad v_b(\eta_b)=\frac{V}{W_b B}(6\eta_b-6\eta_b^2),\\ &\eta_a=\frac{x_a}{W_a},\quad \eta_b=\frac{x_b}{W_b},\quad \xi=\frac{z}{L},\quad Gz=\frac{2VW}{\alpha BL},\\ &\psi_a=\frac{T_a-T_s}{T_I-T_s},\quad \psi_b=\frac{T_b-T_s}{T_I-T_s}\end{aligned}\tag{22}$$

The boundary conditions for solving Eqs. (20) and (21) are

$$\psi_a(0,\xi)=0\tag{23}$$

$$\psi_a(1,\xi)=\psi_b(1,\xi)\tag{24}$$

$$-\frac{\partial\psi_a(1,\xi)}{\partial\eta_a}=\frac{W_a}{W_b}\frac{\partial\psi_b(1,\xi)}{\partial\eta_b}\tag{25}$$

$$\psi_b(0,\xi)=0\tag{26}$$

The mathematical manipulation is similar to that in the previous section, the results of dimensionless outlet temperatures for double-pass devices are

$$\psi_F = \frac{-\int_0^1 v_b W_b B \psi_b(\eta_b, 0)\,\mathrm{d}\eta_b}{V} = \frac{-W}{GzW_b}\sum_{m=0}^{\infty}\frac{S_{b,m}\mathrm{e}^{-\lambda_m}}{\lambda_m}\{F'_{b,m}(1) - F'_{b,m}(0)\} \quad (27)$$

or

$$\psi_F = \left[\frac{\alpha BL}{W_a}\sum_{m=0}^{\infty} S_{a,m}F'_{a,m}(0)\int_0^1 \mathrm{e}^{-\lambda_m(1-\xi)}\,\mathrm{d}\xi + \frac{\alpha BL}{W_b}\sum_{m=0}^{\infty} S_{b,m}F'_{b,m}(0)\int_0^1 \mathrm{e}^{-\lambda_m(1-\xi)}\,\mathrm{d}\xi\right] \quad (28)$$

2.3. Temperature distributions in single-pass devices

For the single-pass device of the same size, all three impermeable sheets in Fig. 1(a) are removed. The velocity distribution and equation of heat transfer in dimensionless form may be written as

$$\frac{\partial^2\psi_0(\eta_0,\xi)}{\partial\eta_0^2} = \left[\frac{W^2 v_0(\eta_0)}{L\alpha}\right]\frac{\partial\psi_0(\eta_0,\xi)}{\partial\xi} \quad (29)$$

$$v_0(\eta_0) = \frac{2V}{WB}(6\eta_0 - 6\eta_0^2), \quad 0 \leqslant \eta_0 \leqslant 1 \quad (30)$$

in which

$$\eta_0 = \frac{x}{W}, \quad \xi = \frac{z}{L}, \quad Gz = \frac{2VW}{\alpha BL}, \quad \psi_0 = \frac{T_0 - T_s}{T_I - T_s} \quad (31)$$

The boundary conditions for solving Eq. (29) are

$$\psi_0(0,\xi) = 0 \quad (32)$$

$$\psi_0(1,\xi) = 0 \quad (33)$$

The calculation procedure for a single-pass device is much simpler than that for a double- or multi-pass device. The result of the outlet temperature is

$$\theta_{0,F} = 1 - \psi_{0,F} = \frac{1}{Gz}\sum_{m=0}^{\infty}\left[\frac{(1-\mathrm{e}^{-\lambda_{0,m}})}{\lambda_{0,m}}S_{0,m}F'_{0,m}(0) - \frac{(1-\mathrm{e}^{-\lambda_{0,m}})}{\lambda_{0,m}}S_{0,m}F'_{0,m}(1)\right] \quad (34)$$

3. Heat transfer efficiency improvement

The Nusselt number for multi-pass device by inserted impermeable sheets may be obtained as follows:

$$\overline{Nu} = \frac{\overline{h}W}{k} \quad (35)$$

in which the average heat-transfer coefficient is defined as

$$\overline{h}(2BL)(T_s - T_I) = 2V\rho c_p(T_F - T_I) \quad (36)$$

or

$$\overline{h} = \frac{2V\rho c_p}{2BL}\left(\frac{T_F - T_I}{T_s - T_I}\right) = \frac{2V\rho c_p}{2BL}(1 - \psi_F) \quad (37)$$

thus

$$\overline{Nu} = \frac{\overline{h}W}{k} = \frac{2VW}{2\alpha BL}(1-\psi_F) = 0.5Gz(1-\psi_F) \quad (38)$$

Similarly, for a single-pass device without recycle

$$\overline{Nu_0} = \frac{\overline{h_0}W}{k} = \frac{2VW}{2\alpha BL}(1-\psi_{0,F}) = 0.5Gz(1-\psi_{0,F}) = 0.5Gz\theta_{0,F} \quad (39)$$

The heat transfer efficiency improvement, I_h, for double- and four-pass devices by inserting the impermeable sheet with negligible thermal resistance is best illustrated by calculating the percentage increase in heat-transfer rate, based on the heat transfer of a single-pass operation of the same Graetz number without recycle as

$$I_h = \frac{\overline{Nu} - \overline{Nu_0}}{\overline{Nu_0}}\% \quad (40)$$

4. Numerical examples

4.1. Power consumption increment

The laminar flow in all subchannels of multi-pass operations is assumed, the power consumption increment, I_p, due to the friction losses ($\ell w_{f,a}$, $\ell w_{f,b}$, $\ell w_{f,c}$ and $\ell w_{f,d}$ for multi-pass devices while $\ell w_{f,0}$ for single-pass devices) in the flow channel can readily derived as [15]

$$I_p = \frac{P - P_0}{P_0} = \frac{[(R+1)\ell w_{f,a} + R\ell w_{f,b} + R\ell w_{f,c} + (R+1)\ell w_{f,d}] - (2\ell w_{f,0})}{2\ell w_{f,0}} \quad (41)$$

$$= \frac{1}{4}(R+1)^2\left(\frac{W}{W_a}\right)^3 + \frac{1}{4}R^2\left(\frac{W}{W_b}\right)^3 + \frac{1}{4}R^2\left(\frac{W}{W_c}\right)^3 + \frac{1}{4}(R+1)^2\left(\frac{W}{W_d}\right)^3 - 1 \quad (42)$$

where $P = V\rho[(R+1)\ell w_{f,a} + R\ell w_{f,b} + R\ell w_{f,c} + (R+1)\ell w_{f,d}]$ and $lw_{f,i} = (2f\overline{v_i}^2 L)/D_h$, $i = 0, a, b, c$ or d. As an illustration, the power consumption of the single-pass device will be illustrated by the working dimensions as follows: $L = 1.2$ m, $W = 0.04$ m, $B = 0.2$ m, $V = 1\times10^{-5}$ m^3/s, $\mu = 8.94\times10^{-4}$ kg/ms, $\rho = 997.08$ kg/m^3. From those numerical values, the friction loss and hydraulic dissipated energy P_0 in a open conduit of a single-pass device

was calculated by the appropriate equations and the results are

$$P_0 = 2V\rho(\ell w_{\mathrm{f},0}) = (2V)f\frac{4L}{D_\mathrm{h}}\left(\frac{1}{2}\rho\bar{v}^2\right) = 1.073\times10^{-4}\ \mathrm{W} = 1.44\times10^{-7}\ \mathrm{hp} \quad (43)$$

Some results for I_p of multi-pass device are presented in Table 1.

4.2. Case studies of heat transfer efficiency improvement

The recycle effect on heat-transfer efficiency improvement was illustrated by the following case studies. Consider the heat transfer for a fluid flowing through a parallel-plate channel with $W = 0.04$ m, $B = 0.2$ m and $\beta_{ab} = \beta_{cd} = 1$.

Case 1: Pure water of 62 °C is flowing through parallel-plate channel with constant wall temperature of 16 °C. The numerical values are assigned as

$$T_\mathrm{I} = 62\ ^\circ\mathrm{C}, \quad T_\mathrm{s} = 16\ ^\circ\mathrm{C},$$
$$\alpha_{\mathrm{water}} = 1.524\times10^{-7}\mathrm{m}^2/\mathrm{s}$$

Case 2: Kerosene at 62 °C is flowing through parallel-plate channel with constant wall temperature of 16 °C. The numerical values are assigned as

Table 1
The power consumption increment with recycle ratio and channel thickness ratio as parameters

R	I_p		
	$\beta_{ab} = \beta_{cd} = 1/3$	$\beta_{ab} = \beta_{cd} = 1$	$\beta_{ab} = \beta_{cd} = 3$
0.5	577.38	79	84.41
1.0	1032.52	159	293.07
2.0	2341.07	415	1108.81
5.0	9452.93	1951	6741.61

Table 2
The results of Case 1

$L\times10^2$ (m)	$V\times10^5$ (m^3/s)	Gz	Nu_0	I_h (%)		
				$R = 0.5$	$R = 3$	$R = 5$
7.8	1.5	50	1.93	4.74	4.70	4.62
	7.5	250	2.00	5.26	5.31	5.34
	3.0	1000	2.02	5.38	5.42	5.44
15.6	1.5	25	1.80	4.20	4.10	3.91
	7.5	125	1.98	5.11	5.13	5.13
	3.0	500	2.02	5.31	5.39	5.41
23.4	1.5	12.5	1.60	3.28	3.10	2.95
	7.5	62.5	1.95	4.83	4.81	4.78
	3.0	250	2.00	5.26	5.31	5.34

Table 3
The results of Case 2

$L\times10^2$ (m)	$V\times10^5$ (m^3/s)	Gz	Nu_0	I_h (%)		
				$R = 1$	$R = 2$	$R = 5$
1.35	1.5	50	1.93	4.74	4.74	4.70
	7.5	250	2.00	5.26	5.26	5.31
	30	1000	2.02	5.38	5.38	5.42
2.7	1.5	25	1.80	4.20	4.20	4.10
	7.5	125	1.98	5.11	5.11	5.13
	30	500	2.02	5.31	5.31	5.39
4.05	1.5	12.5	1.60	3.28	3.28	3.10
	7.5	62.5	1.95	4.83	4.83	4.81
	30	250	2.00	5.26	5.26	5.31

$T_I = 62\ ^\circ C, \quad T_s = 16\ ^\circ C,$

$\alpha_{kerosene} = 8.645 \times 10^{-8} m^2/s$

From these numerical values, the transfer efficiency improvements in laminar counterflow multi-pass coolers operated with external refluxes under various flow rates of fluid and reflux ratios, were calculated by the appropriate equations and the results are presented in Tables 2 and 3.

5. Results and discussion

By following the same mathematical treatment performed in multi-pass parallel-plate heat exchangers of the previous work [15], the temperature distributions in four subchannels were obtained by solving Eq. (2) analytically with the use of Eqs. (4)–(11), while the results were obtained by using the same method to solve Eqs. (20) and (21), and Eq. (29) for single- and double-pass devices, respectively. Finally, the outlet temperatures, referred to the bulk temperatures, are derived from the overall energy balances. As an illustration, some calculation results of the first two eigenvalues and their associated expansion coefficients as well as the dimensionless outlet temperatures were calculated for $\beta_{ab} = \beta_{cd} = 1$, $R = 1$ and $Gz = 1$, 10, 100 and 1000. It appears from Table 4 that only the first negative eigenvalue is necessary to be considered during the calculation of temperature distributions due to the rapid convergence. The value of $Gz\lambda_0$ in multi-pass devices with external refluxes for $\beta_{ab} = \beta_{cd} = 1$ and $R = 1$ is -7.8539, as shown in Table 4, while that in the double-pass devices without recycle is -8.8300. Thus, the eigenvalues are different between the multi- and double-pass devices.

Table 1 shows that the power consumption increment increases with the reflux ratio or as β_{ab} and β_{cd} move away from 1. Although the power consumption increment in multi-pass operations may be large as 9452.93 for $R = 5$ and $\beta_{ab} = \beta_{cd} = 1/3$, however, the power consumption in the single-pass device is extremely small as 1.44×10^{-7} hp. Therefore, the power consumption in all devices may be ignored.

5.1. Heat transfer efficiencies in multi-pass devices

Figs. 2 and 3 show the theoretical dimensionless inlet temperature θ_a (or θ_d) of the fluid after mixing the outlet θ_F, with the reflux ratio and channel thickness ratio as parameters, respectively. The mixed inlet temperature increases with the residence time, which is inversely proportional to the inlet volumetric flow rate. Accordingly, the mixed inlet temperature increases with increasing the reflux ratio, but with decreasing the channel thickness ratio and Graetz number.

Figs. 4 and 5 show the dimensionless outlet temperature θ_F vs. Gz with the reflux ratio and channel thickness ratio as parameters, respectively. The application of recycle-effect concept to improve the performance in coolers or heaters creates two conflict effects: the desirable effect of enhancing convective transfer rate and undesirable one of decreasing the temperature gradient between the fluid and walls. At low Graetz number (either small inlet volumetric flow rate V or large channel length L) the desirable convective transfer rate enhancement by increasing the reflux ratio cannot compensate for the temperature gradient decrement, and hence the devices with external refluxes are not favorable to heat transfer, as shown in Fig. 4 and 5, the dimensionless outlet temperature increases with decreasing the reflux ratio. However, the recycle effect contributes a positive influence on the heat transfer for large Graetz number. This is due to the convective transfer effect having more contribution than the temperature gradient effect here.

5.2. Heat transfer efficiency improvement based on single-pass devices

Fig. 6 shows the theoretical average Nusselt numbers, $\overline{Nu}$ and $\overline{Nu}_0$, with the reflux ratio as a parameter for

Table 4
Eigenvalues and expansion coefficients as well as dimensionless outlet temperatures in multi-pass devices with recycle for $\beta_{ab} = \beta_{cd} = 1$ and $R = 1$; $Gz\lambda_0 = -7.8539$ and $Gz\lambda_1 = -21.485$

Gz	m	λ_m	$S_{a,m}$	$S_{b,m}$	$S_{c,m}$	$S_{d,m}$	$\psi_F(\lambda_1)$	$\psi_F(\lambda_1, \lambda_2)$
1	0	−7.8539	7.6×10^{-4}	2.2×10^{-4}	2.2×10^{-4}	7.6×10^{-4}	0.0003	0.0003
	1	−21.485	-2.8×10^{-25}	-5.8×10^{-20}	-5.8×10^{-20}	-2.8×10^{-25}		
10	0	−0.7854	1.0300	2.9×10^{-1}	2.9×10^{-1}	1.0300	0.3740	0.3740
	1	−2.1485	-7.5×10^{-17}	2.7×10^{-17}	2.7×10^{-17}	-7.5×10^{-17}		
100	0	−0.0785	2.4709	7.0×10^{-1}	7.0×10^{-1}	2.4709	0.8972	0.8972
	1	−0.2149	2.5×10^{-16}	-5.1×10^{-17}	$-5.\ 1\times10^{-17}$	2.5×10^{-16}		
1000	0	−0.0079	2.7239	7.8×10^{-1}	7.8×10^{-1}	2.7239	0.9891	0.9891
	1	−0.0215	-3.8×10^{-15}	4.0×10^{-17}	$4.\ 0\times10^{-17}$	-3.8×10^{-15}		

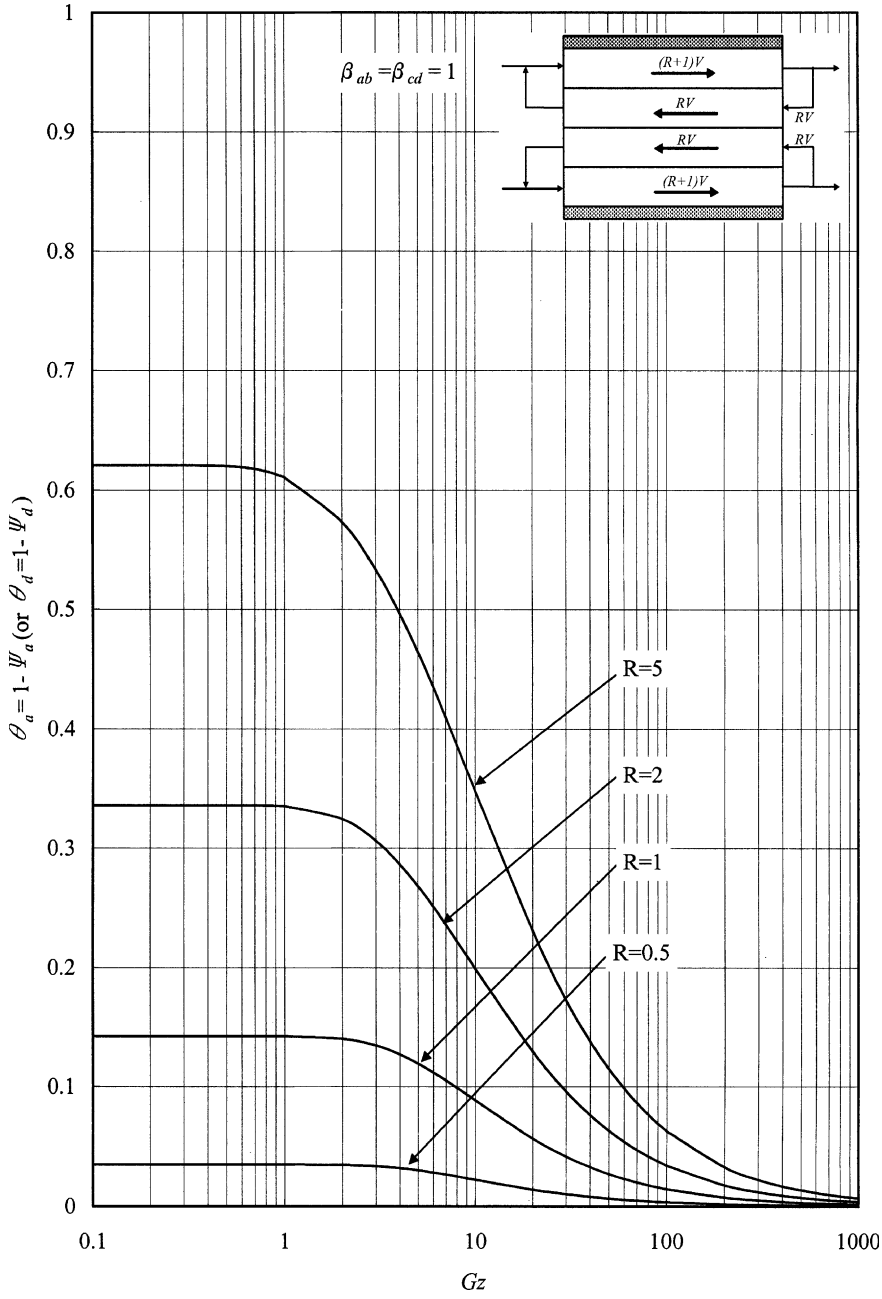

Fig. 2. Dimensionless mixed inlet temperatures of fluid after mixing with recycle ratio as a parameter; $\beta_{ab} = \beta_{cd} = 1$.

$\beta_{ab} = \beta_{cd} = 1$ while Fig. 7 with reflux ratio and channel thickness ratio, β_{ab} and β_{cd}, as parameters. Nusselt numbers and the heat-transfer efficiency improvement are proportional to θ_F ($\theta_{0,F}$), as shown in Eqs. (35) and (36), so the higher improvement of device performance is thus obtained in multi-pass operations with external refluxes.

The improvement percentage of heat transfer efficiency I_h was represented in Table 5 with the Graetz number Gz, channel thickness ratios (β_{ab} and β_{cd}) and recycle ratio R as parameters. It is observed from Table 5 that the average Nusselt numbers increase with Graetz number Gz and recycle ratio R for large Graetz number but with decreasing the channel thickness ratios (β_{ab} and β_{cd}).

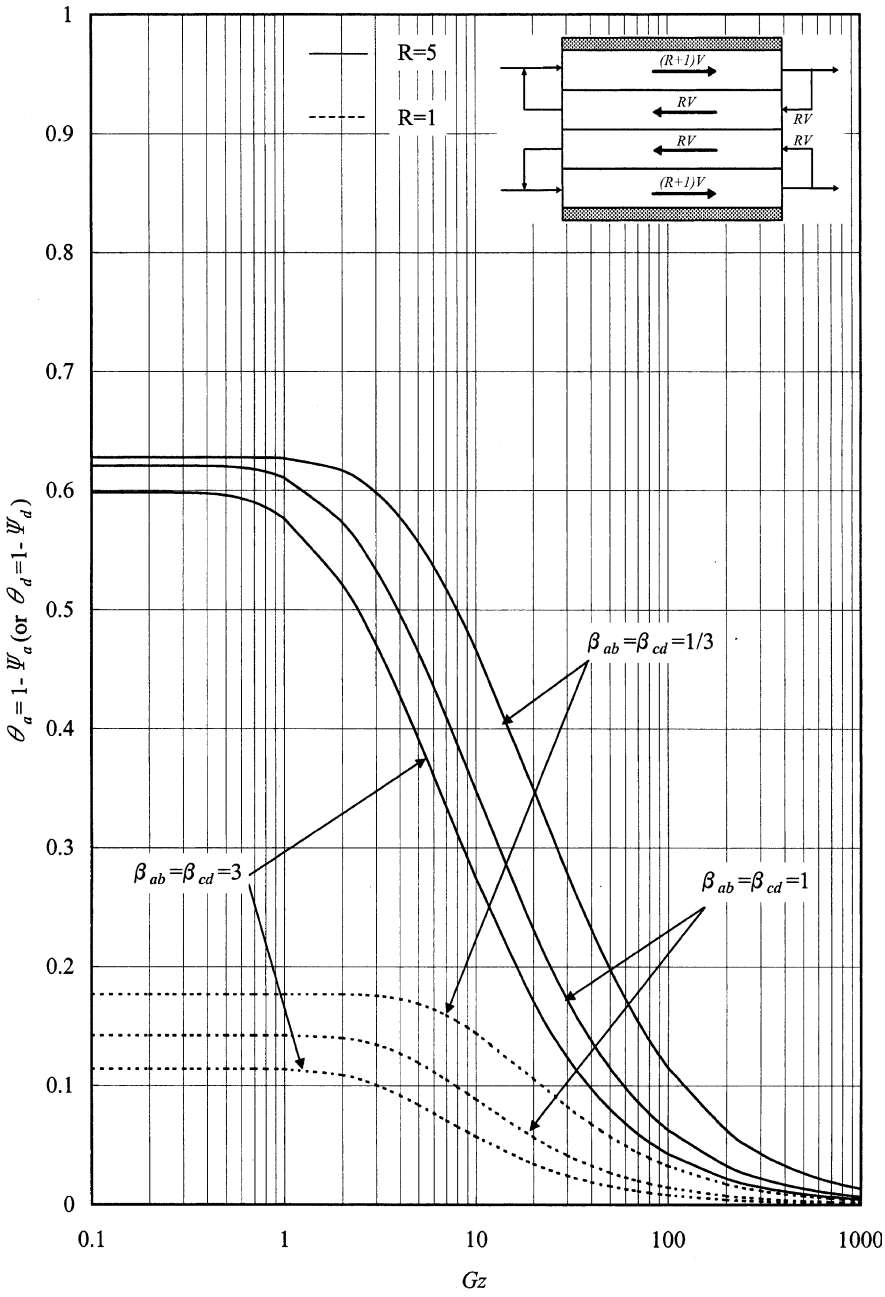

Fig. 3. Dimensionless mixed inlet temperatures of fluid after mixing with channel thickness ratio as a parameter; $R = 1$ and 5.

Two case studies were illustrated for the heat transfer efficiency improvement and the results are shown in Tables 2 and 3. From these two tables we see that I_h increases with Gz and with R. For low Graetz number (large L or small V), a higher improvement percentage is obtained, and I_h decreases as we proceed down Tables 2 and 3.

6. Conclusion

The equation of heat transfer in multi-pass coolers or heaters with external refluxes was developed using the orthogonal expansion technique with the eigenfunctions expanding in terms of an extended power series. When a single-pass parallel-plate cooler or heater is rearranged

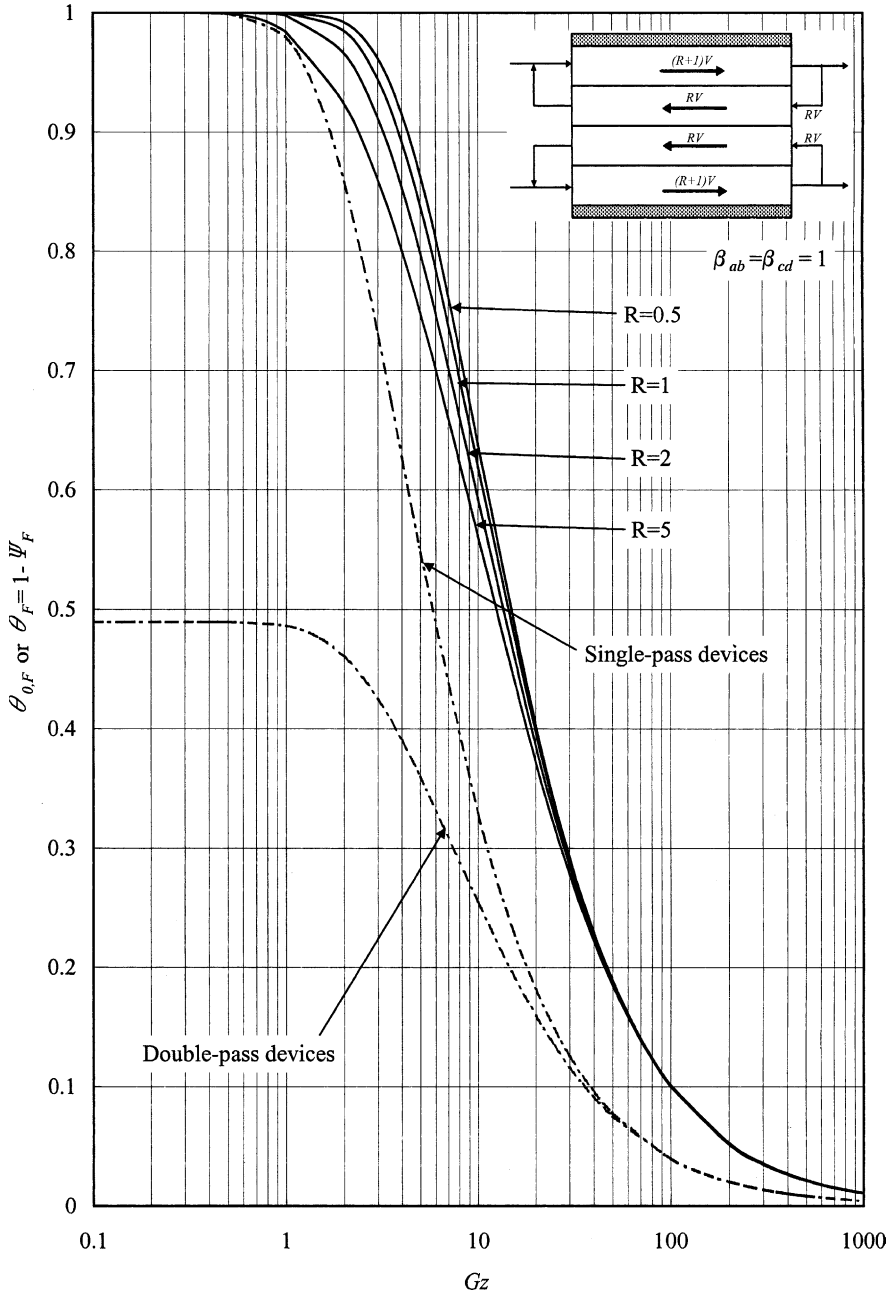

Fig. 4. Dimensionless outlet temperature vs. Gz with recycle ratio as a parameter; $\beta_{ab} = \beta_{cd} = 1$.

to become a multi-pass device, the fluid velocities in each subchannel increase, thereby leading to increased convective heat transfer rate. It is concluded that the application of recycle-effect concept in a parallel-plate conduit can enhance heat transfer for fluid flowing through multi-pass coolers or heaters by inserting impermeable sheets with negligible thermal resistance. The local transversal temperature profile in channels a and b, for $\beta_{ab} = \beta_{cd} = 1$ and $R = 1$ and for various axial distance ξ presented in Fig. 8 lend credibility to the theoretical predictions of the mathematical model. The present study is actually the extension of our previous work [15] except the type of reflux. Fig. 9 illustrates the graphical representation for comparisons with the same parameter values used in Fig. 7 to explain how the present recycle device improves on the previous work. It is observed in Fig. 9 that the average Nusselt number of the present work is higher than that in our previous

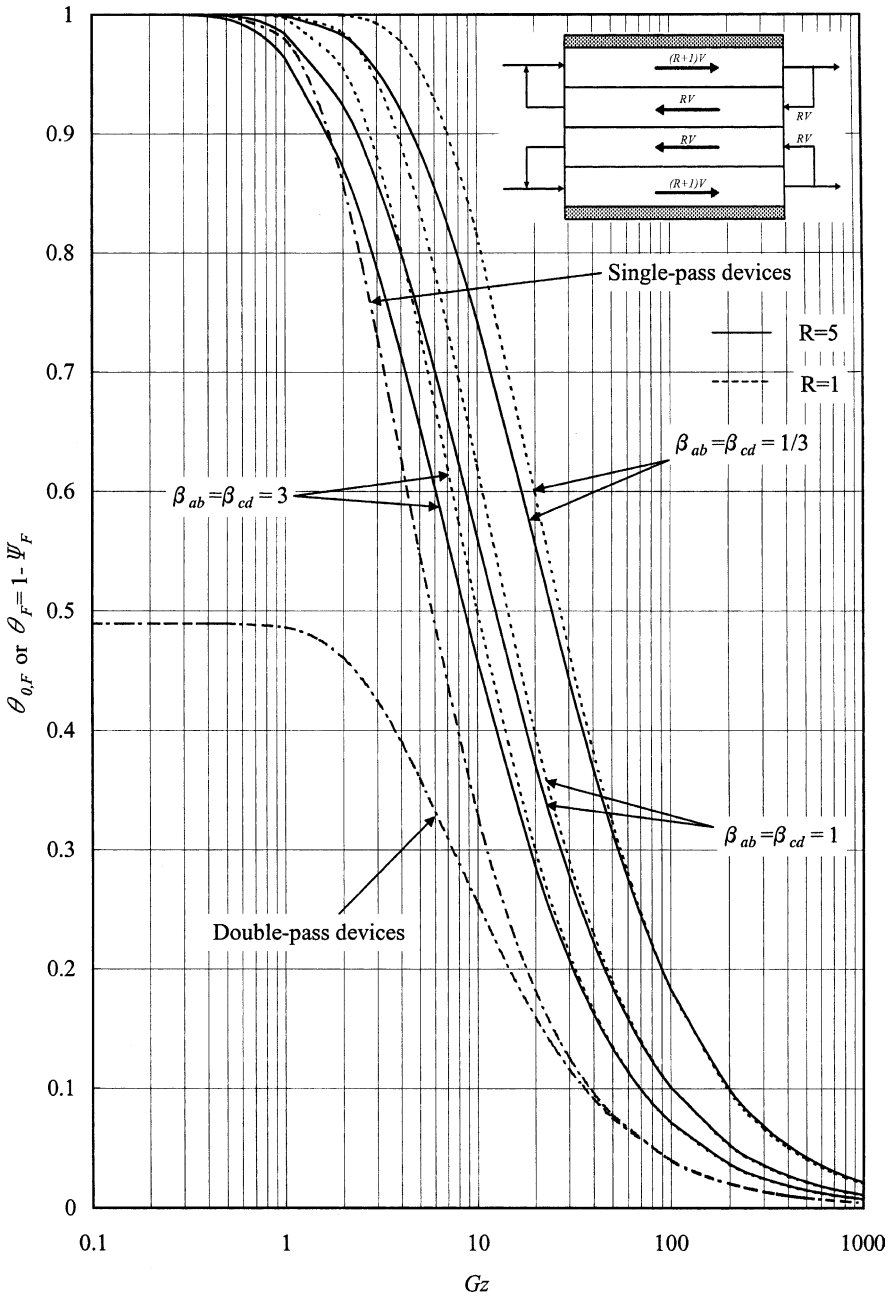

Fig. 5. Dimensionless outlet temperature vs. Gz with channel thickness ratio as a parameter; $R = 1$ and 5.

work [15], which the contribution differs from the previous work. With those comparisons, the advantage of present devices is evident for any Graetz numbers with $R = 5$.

Considerable improvement in heat transfer is obtainable if a cooler or heater is operated with external refluxes, which provide the preheating effect and the enlargement in fluid velocity. However, the increases in operating cost should be taken into account with the economic sense. Therefore, both the heat transfer improvement, I_h, and the power consumption increment, I_p, were considered in economical feasibility to suitably select the design parameter (β_{ab} and β_{cd}) and the operating parameters (Gz and R). The results of I_h/I_p with recycle ratio and channel thickness ratio as parameters were presented in Fig. 10. Fig. 10 shows that the values

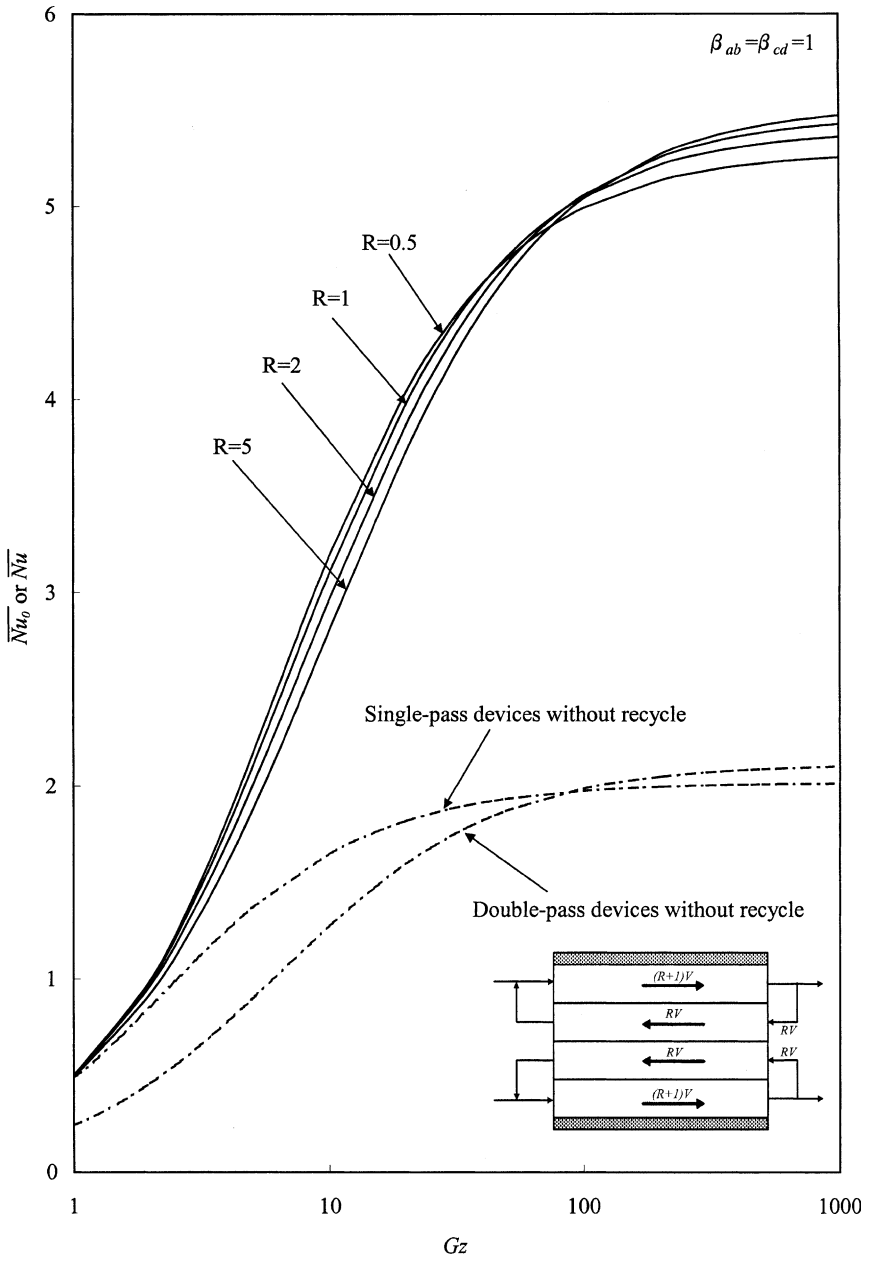

Fig. 6. Average Nusselt number vs. Gz with recycle ratio as a parameter; $\beta_{ab} = \beta_{cd} = 1$.

of I_h/I_p decrease with increasing the recycle ratio and as the channel thickness ratio (β_{ab} and β_{cd}) moves away from 1, especially for $\beta_{ab} = \beta_{cd} > 1$ with $Gz > 20$.

Acknowledgements

The author wishes to thank the National Science Council of the Republic of China for its financial support.

Appendix A

By using the method of separation of variables, the dimensionless temperature can be written in the form

$$\psi_i(\eta_i, \xi) = \sum_{m=0}^{\infty} S_{i,m} F_{i,m}(\eta_i) G_m(\xi) \quad i = a, b, c, d \tag{A.1}$$

and applied to Eqs. (2) and (3) leading to

$$G_m(\xi) = e^{-\lambda_m(1-\xi)} \tag{A.2}$$

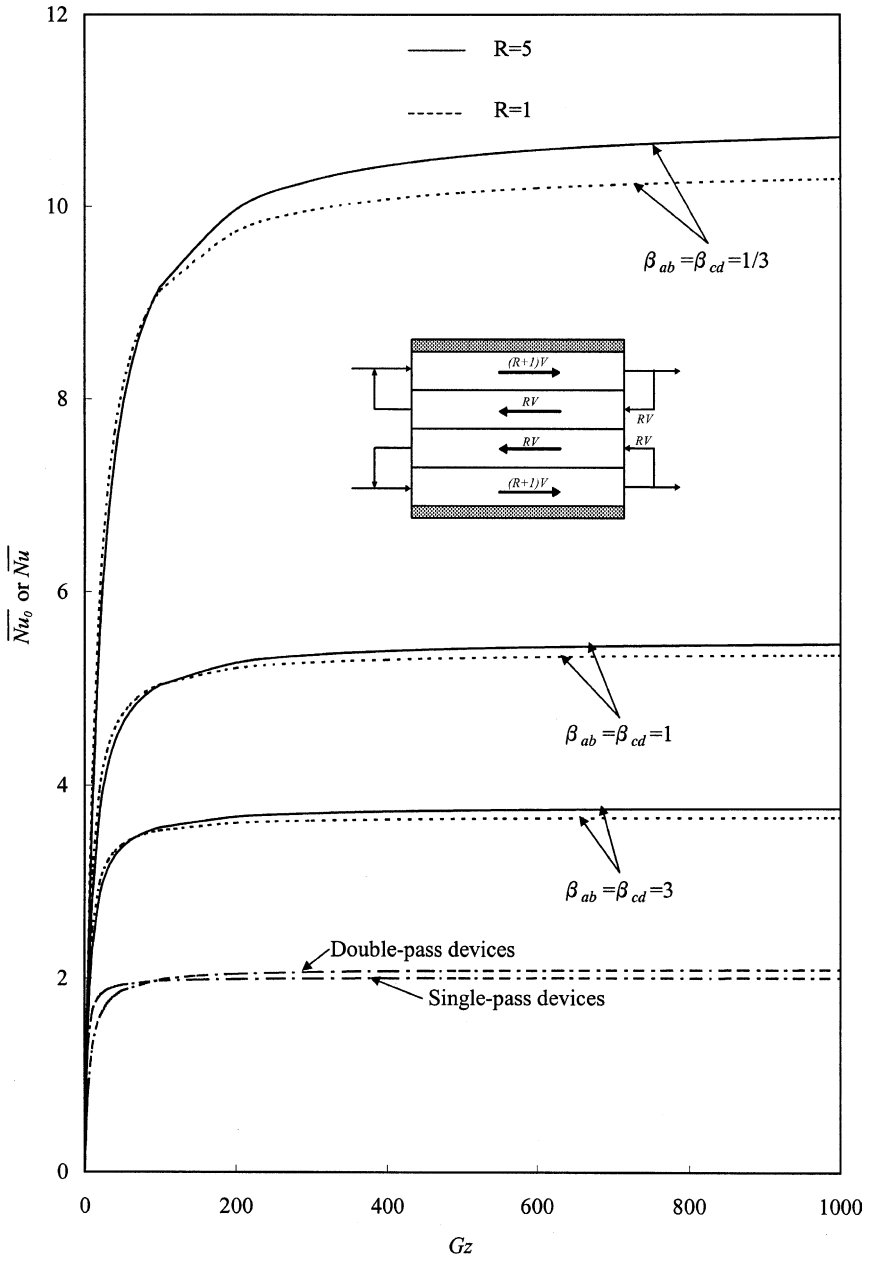

Fig. 7. Average Nusselt number vs. Gz with channel thickness ratio as a parameter; $R = 1$ and 5.

$$F''_{i,m}(\eta) - \left[\frac{\lambda_m W_i^2 v_i(\eta_i)}{LD}\right] F_{i,m}(\eta) = 0 \quad i = a, b, c, d \tag{A.3}$$

as well as the boundary conditions in Eqs. (4)–(11) can be rewritten as

$$F_{a,m}(0) = 0 \tag{A.4}$$

$$S_{a,m}F_{a,m}(1) = S_{b,m}F_{b,m}(1) \tag{A.5}$$

$$S_{a,m}F'_{a,m}(1) = -\frac{W_a}{W_b}S_{b,m}F'_{b,m}(1) \tag{A.6}$$

$$S_{b,m}F_{b,m}(0) = S_{c,m}F_{c,m}(0) \tag{A.7}$$

$$S_{b,m}F'_{b,m}(0) = -\frac{W_b}{W_c}S_{c,m}F'_{c,m}(0) \tag{A.8}$$

$$S_{c,m}F_{c,m}(1) = S_{d,m}F_{d,m}(1) \tag{A.9}$$

Table 5
The improvement of the transfer efficiency with reflux ratio and channel thickness ratio as parameters

I_h (%)	$\beta_{ab}=\beta_{cd}=1/3$	$\beta_{ab}=\beta_{cd}=1$	$\beta_{ab}=\beta_{cd}=3$
$R=1$			
$Gz=1$	2.15	2.12	1.89
$Gz=10$	147.49	88.07	51.44
$Gz=100$	361.97	155.32	78.70
$Gz=1000$	410.70	166.14	82.48
$R=2$			
$Gz=1$	2.15	1.93	1.21
$Gz=10$	136.91	79.86	46.09
$Gz=100$	360.38	155.80	80.16
$Gz=1000$	417.63	169.45	85.43
$R=3$			
$Gz=1$	2.04	0.53	−1.55
$Gz=10$	125.67	70.24	39.14
$Gz=100$	363.88	154.99	80.23
$Gz=1000$	432.18	171.67	87.13

$$S_{c,m}F'_{c,m}(1)=-\frac{W_c}{W_d}S_{d,m}F'_{c,m}(1) \tag{A.10}$$

$$F_{d,m}(0)=0 \tag{A.11}$$

where the primes on $F_{a,m}(\eta_a)$, $F_{b,m}(\eta_b)$, $F_{c,m}(\eta_c)$ and $F_{d,m}(\eta_d)$ denote the differentiations with respect to η_a, η_b, η_c and η_d, respectively.

Combinations of Eqs. (A.5) and (A.6), Eqs. (A.7) and (A.8), and Eqs. (A.9) and (A.10) result in Eqs. (A.12), (A.13), (A.14), respectively

$$\frac{F_{a,m}}{F'_{a,m}}=-\frac{W_bF_{b,m}(1)}{W_aF'_{b,m}(1)} \tag{A.12}$$

$$\frac{F_{b,m}}{F'_{b,m}}=-\frac{W_cF_{c,m}(0)}{W_bF'_{c,m}(0)} \tag{A.13}$$

$$\frac{F_{c,m}}{F'_{c,m}}=-\frac{W_dF_{d,m}(1)}{W_cF'_{d,m}(1)} \tag{A.14}$$

To avoid the loss of generality, the eigenfunctions $F_{a,m}(\eta_a)$, $F_{b,m}(\eta_b)$, $F_{c,m}(\eta_c)$ and $F_{d,m}(\eta_d)$ were assumed to be polynomials. By using Eqs. (A.4) and (A.11), we can get

$$F_{a,m}(\eta_a)=\sum_{n=0}^{\infty}p_{m,n}\eta_a^n,\quad p_{m,0}=0,\quad p_{m,1}=1\ \text{(selected)} \tag{A.15}$$

$$F_{b,m}(\eta_b)=\sum_{n=0}^{\infty}q_{m,n}\eta_b^n,\quad q_{m,0}=1\ \text{(selected)} \tag{A.16}$$

$$F_{c,m}(\eta_c)=\sum_{n=0}^{\infty}r_{m,n}\eta_c^n,\quad r_{m,0}=1\ \text{(selected)} \tag{A.17}$$

$$F_{d,m}(\eta_d)=\sum_{n=0}^{\infty}t_{m,n}\eta_d^n,\quad t_{m,0}=0,\quad t_{m,1}=1\ \text{(selected)} \tag{A.18}$$

Substitution of the Eqs. (A.15)–(A.18) into Eq. (A.3) will lead to all of the coefficients $p_{m,n}$, $q_{m,n}$, $r_{m,n}$ and $t_{m,n}$ to be in terms of eigenvalues λ_m after using Eqs. (A.4) and (A.11). The dimensionless outlet temperature $\psi_{F,ab}$ or $\psi_{F,cd}$ can be obtained as Eq. (13) or (14) while all of the eigenvalues (λ_m), the expansion coefficients, ($S_{a,m}$, $S_{b,m}$, $S_{c,m}$ and $S_{d,m}$) and the associated eigenfunctions ($F_{a,m}$, $F_{b,m}$, $F_{c,m}$ and $F_{d,m}$) are found.

References

[1] R.K. Shah, A.L. London, Laminar Flow Forced Convection in Ducts, Academic Press, New York, 1978, pp. 196–207.
[2] V.-D. Dang, M. Steinberg, Convective diffusion with homogeneous and heterogeneous reaction in a tube, J. Phys. Chem. 84 (1980) 214–219.
[3] B. Weigand, An extract analytical solution for the extended turbulent Graetz problem with prescribed with Dirichlet wall boundary conditions for pipe and channel flows, Int. J. Heat Mass Transfer 39 (1996) 1625–1637.
[4] J.R. Sellars, M. Tribus, J.S. Klein, Heat transfer to laminar flow in a round tube or flat conduit—the Graetz problem extended, Trans. Am. Soc. Mech. Engrs. 78 (1956) 441–448.
[5] A.P. Hatton, A. Quarmby, Heat transfer in the thermal entry length with laminar flow in an annulus, Int. J. Heat Mass Transfer 5 (1962) 973–980.
[6] T.L. Perelman, On conjugated problems of heat transfer, Int. J. Heat Mass Transfer 3 (1961) 293–303.

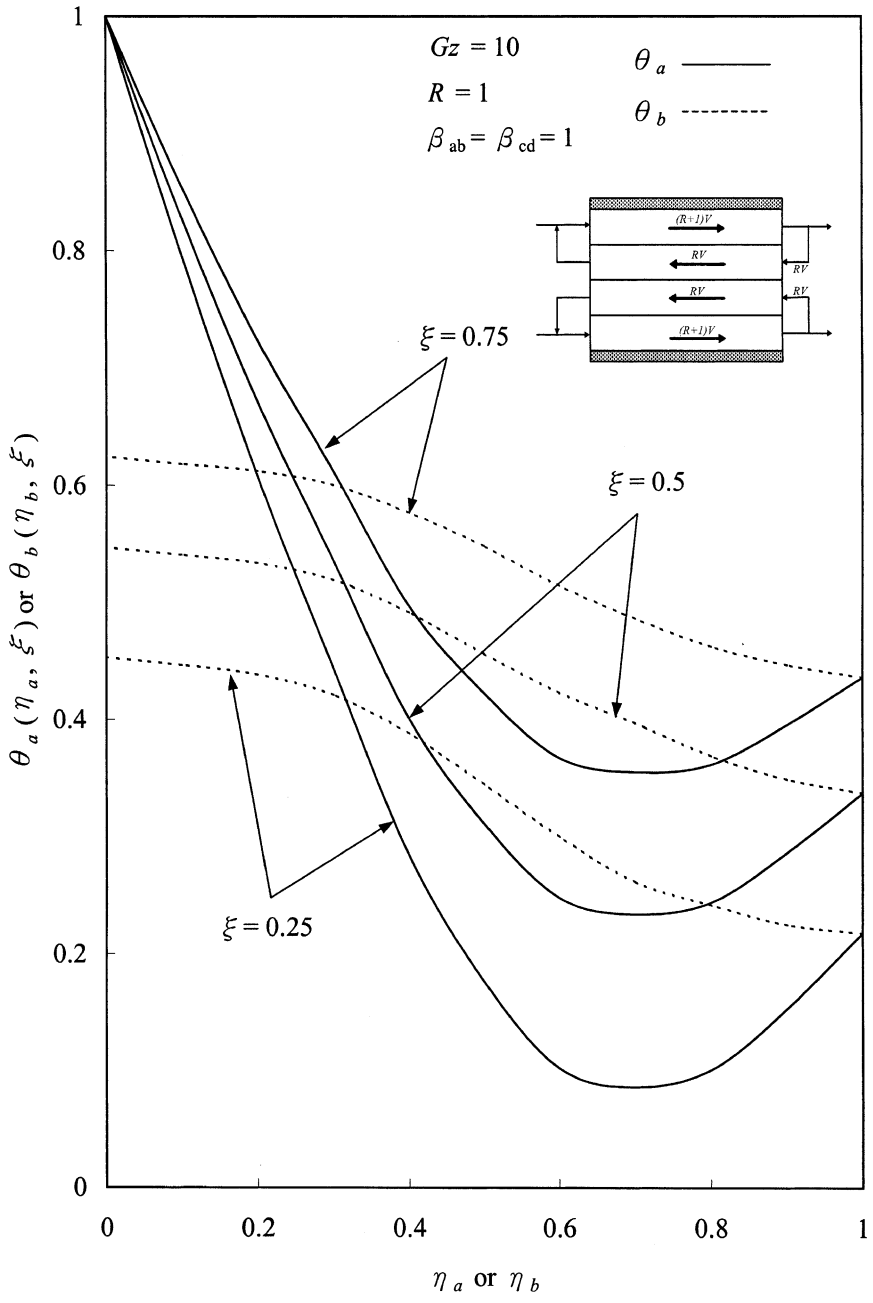

Fig. 8. The local transversal temperature in channels a and b, for $Gz = 10$, $\beta_{ab} = \beta_{cd} = 1$ and $R = 1$ and for various axial distance ξ.

[7] D. Murkerjee, E.J. Davis, Direct-contact heat transfer immiscible fluid layers in laminar flow, AIChE J. 18 (1972) 94–101.
[8] S.S. Kim, D.O. Cooney, Improved theory for hollow-fiber enzyme reactor, Chem. Eng. Sci. 31 (1976) 289–294.
[9] E.J. Davis, S. Venkatesh, The solution of conjugated multiphase heat and mass transfer problems, Chem. Eng. Sci. 34 (1979) 775–787.
[10] E. Papoutsakis, D. Ramkrishna, Conjugated Graetz problems. I: general formalism and a class of solid–fluid problems, Chem. Eng. Sci. 36 (1981) 1381–1390.
[11] E. Papoutsakis, D. Ramkrishna, Conjugated Graetz problems. II: fluid–fluid problems, Chem. Eng. Sci. 36 (1981) 1393–1399.
[12] X. Yin, H.H. Bau, The conjugated Graetz problem with axial conduction, Trans. ASME 118 (1996) 482–485.

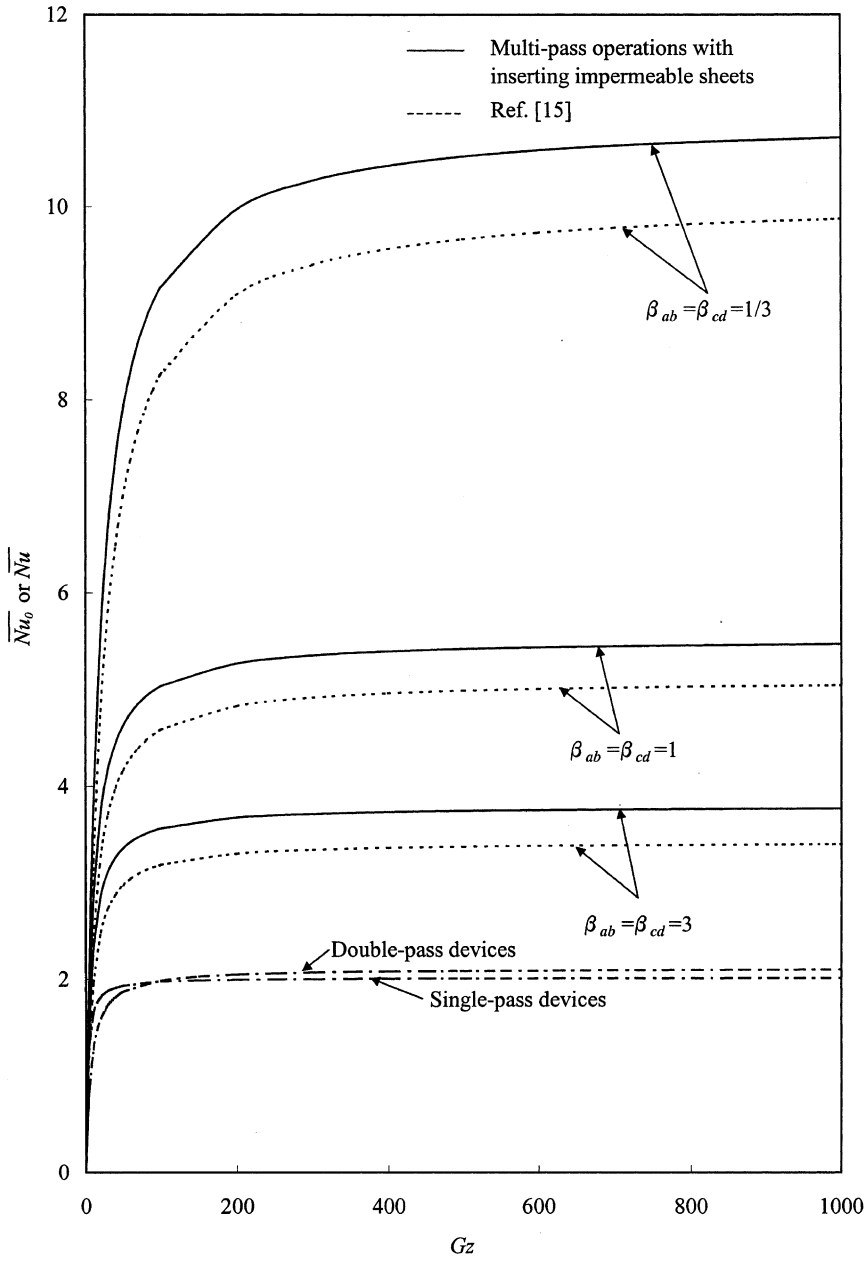

Fig. 9. Average Nusselt number of both multi-pass devices in the previous [15] and present work vs. Gz with channel thickness ratio as a parameter; $R = 5$.

[13] R.J. Nunge, W.N. Gill, Analysis of heat and mass transfer in some countercurrent flows, Int. J. Heat Mass Transfer 8 (1965) 873–886.
[14] H.M. Yeh, S.W. Tsai, T.W. Chang, A study of the Graetz problem in concentric-tube continuous-contact countercurrent separation processes with recycles at both ends, Sep. Sci. Technol. 21 (1986) 403–419.
[15] C.D. Ho, H.M. Yeh, Y.C. Tsai, Improvement in performance of multi-pass laminar counterflow heat exchangers with external refluxes, Int. J. Heat Mass Transfer 45 (2002) 3529–3547.
[16] C.D. Ho, H.M. Yeh, J.J. Guo, An analytical study on the enrichment of heavy water in the continuous thermal-diffusion column with external refluxes, Sep. Sci. Technol. 37 (2002) 3129–3153.
[17] E. Santacesaria, M. Di Serio, P. Iengo, Mass transfer and kinetics in ethoxylation spray tower loop reactors, Chem. Eng. Sci. 54 (1999) 1499–1504.

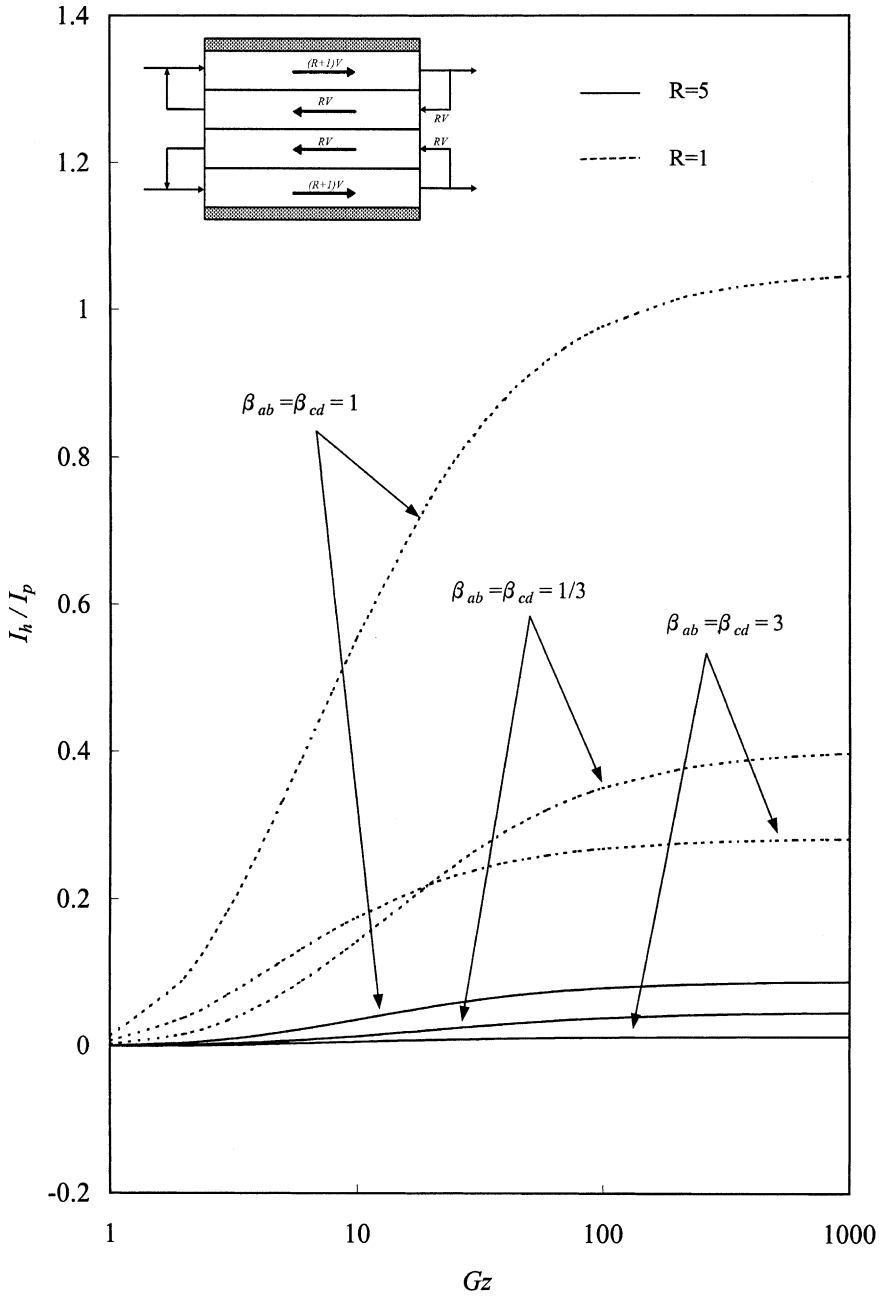

Fig. 10. The values of I_h/I_p vs. Gz with channel thickness ratio as a parameter; $R = 1$ and 5.

[18] R. Marquart, Circulation of high-viscosity newtonian and non-newtonian liquids in jet loop reactor, Int. Chem. Eng. 20 (1981) 399–407.

[19] E. Garcia-Calvo, A. Rodriguez, A. Prados, J. Klein, Fluid dynamic model for three-phase airlift reactors, Chem. Eng. Sci. 54 (1998) 2359–2370.

[20] M. Atenas, M. Clark, V. Lazarova, Holdup and liquid circulation velocity in a rectangular air-lift bioreactor, Ind. Eng. Chem. Res. 38 (1999) 944–949.

[21] S. Goto, P.D. Gaspillo, Effect of static mixer on mass transfer in draft tube bubble column and in external loop column, Chem. Eng. Sci. 47 (1992) 3533–3539.

[22] K.I. Kikuchi, H. Takahashi, Y. Takeda, F. Sugawara, Hydrodynamic behavior of single particles in a draft-tube bubble column, Can. J. Chem. Eng. 77 (1999) 573–578.

[23] S.N. Singh, The determination of eigen-functions of a certain Sturm–Liouville equation and its application to

problems of heat-transfer, Appl. Sci. Res., Sect. A 32 (1958) 237–250.
[24] G.M. Brown, Heat or mass transfer in a fluid in laminar flow in a circular or flat conduit, AIChE J. 6 (1960) 179–183.
[25] R.J. Nunge, W.N. Gill, An analytical study of laminar counterflow double-pipe heat exchangers, AIChE J. 12 (1966) 279–289.
[26] H.M. Yeh, S.W. Tsai, C.S. Lin, A study of the separation efficiency in thermal diffusion columns with a vertical permeable barrier, AIChE J. 32 (1986) 971–980.
[27] M.A. Ebadian, H.Y. Zhang, An exact solution of extended Graetz problem with axial heat conduction, Int. J. Heat Mass Transfer 32 (1989) 1709–1717.